HHS Public Access

Author manuscript

Macromol Biosci. Author manuscript; available in PMC 2019 February 01.

Published in final edited form as:

Macromol Biosci. 2018 February ; 18(2): . doi:10.1002/mabi.201700267.

A Stereolithography-based 3D printed Hybrid Scaffold for *in Situ* Cartilage Defect Repair

Elizabeth A Aisenbrey,
Department of Chemical and Biological Engineering, University of Colorado, Boulder, CO 80309 USA

Andrew Tomaschke,
Department of Mechanical Engineering, University of Colorado, Boulder, CO 80309 USA

Eric Kleinjan,
Department of Chemical and Biological Engineering, University of Colorado, Boulder, CO 80309 USA

Archish Muralidharan,
Material Science and Engineering Program, University of Colorado, Boulder, CO 80309 USA

Dr. Cecilia Pascual-Garrido,
Washington University Orthopedics, Washington University, St. Louis, MO 63110 USA

Prof. Robert R. McLeod,
Department of Electrical, Computing and Energy, Material Science and Engineering Program, University of Colorado, Boulder, CO 80309 USA

Prof. Virginia L. Ferguson, and
Department of Mechanical Engineering, Material Science and Engineering Program, BioFrontiers Institute, University of Colorado, Boulder, CO 80309 USA

Prof. Stephanie J. Bryant
Department of Chemical and Biological Engineering, Material Science and Engineering Program, BioFrontiers Institute, University of Colorado, Boulder, CO 80309 USA

Abstract

Damage to articular cartilage can over time cause degeneration to the tissue surrounding the injury. To address this problem, scaffolds that prevent degeneration and promote neotissue growth are needed. We introduce a new hybrid scaffold that combines a stereolithography-based three-dimensional printed support structure with an injectable and photopolymerizable hydrogel for delivering cells to treat focal chondral defects. In this proof of concept study, we demonstrate the ability to a) infill the support structure with an injectable hydrogel precursor solution, b) incorporate cartilage cells during infilling using a degradable hydrogel that promotes neotissue deposition, and c) minimize damage to the surrounding cartilage when the hybrid scaffold is placed *in situ* in a focal chondral defect in an osteochondral plug that is cultured under mechanical loading. With the ability to independently control the properties of the structure and the injectable hydrogel, this hybrid scaffold approach holds promise for treating chondral defects.

Graphical Abstract

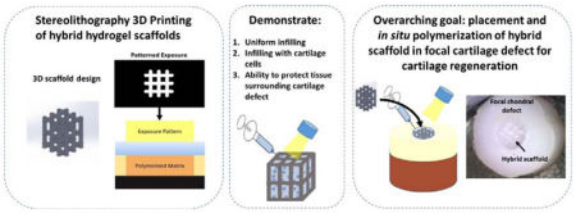

1. Introduction

Focal defects that occur in articular cartilage as a result of injury pose a significant risk for developing osteoarthritis, a debilitating disease with no cure.[1,2] Once damaged, articular cartilage has a limited capacity to self-repair. The lack of repair causes changes to the mechanical environment in the cartilage that surrounds the empty defect,[3] which over time, can lead to degeneration and eventually progress to osteoarthritis. Unfortunately, the only effective solution to treat advanced osteoarthritis is joint arthroplasty. However, if the defect can be repaired while minimizing degeneration to the surrounding tissue, prevention of osteoarthritis may be possible. To this end, microfracture has been widely used to treat focal defects, where small fractures to the underlying subchondral bone induce bleeding and recruit bone marrow cells to facilitate repair.[4,5] Although patient reported outcomes are temporarily improved, microfracture produces a mechanically inferior fibrous tissue that eventually leads to degeneration[4,6,7] and is not suitable for large defects. Cellular therapies based on autologous chondrocyte implantation (ACI) were developed in an effort to improve cartilage repair. Results from ACI treated defects have shown some improvement in the short-term (up to one year),[8] but long-term leads to similar repair[9–13] when compared to microfracture. Taken together, there remains a great need to develop new therapies that are capable of repairing focal defects with functionally competent cartilage tissue and ultimately preventing progression to osteoarthritis.[6,14]

One promising approach combines a hydrogel (i.e., matrix) with ACI to deliver chondrocytes into the defect within a three-dimensional (3D) matrix.[15–19] In particular, hydrogels afford the opportunity to design the 3D environment with biochemical and mechanical cues[20] to support the chondrogenic phenotype.[21,22] Synthetic and degradable hydrogels have been investigated for cartilage regeneration due to the ability to tune the chemistry, mechanical properties, and degradation behavior of the hydrogel and promote cartilage growth.[23,24] Moreover, *in situ* formation of the hydrogel in the defect enables the hydrogel to adhere to the surrounding tissue and ultimately facilitate integration while working as a vehicle for *in situ* cell delivery to promote cartilage regeneration.[25]

Designing a hydrogel that maintains the overall integrity of the construct while allowing for degradation and ECM synthesis of encapsulated cells remains challenging. Cell-laden hydrogels consist of a tight mesh of polymer crosslinks that surround the encapsulated cells. This mesh, which is on the nanometer length scale, restricts transport of the main cartilage ECM macromolecules (i.e., collagen type II and aggrecan) and thus prevents macroscopic neotissue growth.[26] As a result, there is a temporary loss in the structural integrity as the hydrogel degrades, but before sufficient macroscopic tissue can be deposited.[23,27,28] This

loss in structural integrity may compromise the encapsulated cells and damage surrounding cartilage tissue when used *in vivo* to treat focal defects, especially under physiological mechanical forces.

To overcome the shortcomings associated with using a single scaffold design for cell encapsulation, this proof of concept study sought to explore the potential of a new hybrid scaffold whereby a support structure is introduced into the cell-laden hydrogel (Figure 1). The overarching idea is to create a minimally invasive approach based on a hybrid scaffold containing a slow degrading temporary structure that provides support while an infilled fast degrading chondrocyte-laden hydrogel allows for neotissue formation. Collectively, the scaffold should also minimize damage to surrounding cartilage tissue. Stereolithography (SLA) 3D printing was chosen to fabricate the 3D support structure due to its high resolution printing capabilities from photopolymerizable precursors and for its ability to create complex architectures in a layer-by-layer fashion without requiring a sacrificial material.[29–33] A well-established poly(ethylene glycol) (PEG) hydrogel prepared from a step-growth photopolymerization reaction was chosen for the cell-laden hydrogel for its demonstrated promise in cell encapsulation[34] and cartilage tissue engineering.[35,36] Herein, the feasibility of our idea is demonstrated by the ability to infill the 3D support structure with a cell-compatible hydrogel and subsequently support cartilage cells and ECM deposition. Moreover, the *in situ* placement of the hybrid scaffold in an *ex vivo* model of a cartilage focal defect and the ability to protect the surrounding cartilage in a mechanically relevant loading environment are demonstrated.

2. Results and Discussion

The 3D support structure was designed to fulfill several criteria. First, the structure needed to be stable over the course of the experiments to maintain structural integrity. Second, the structure needed to be infilled with the aqueous cell-compatible hydrogel precursor solution and therefore needed to be hydrophilic. And lastly, the structure needed to maintain integrity while having sufficient void space to infill with cells and allow for neotissue deposition. From these criteria, a 3D support structure was designed with an array of evenly spaced 250 μm diameter pillars which were connected together using a lattice structure at the base, middle, and top. The continuous pillar design provided structural support to resist compressive forces, while the lattice provided lateral support to resist transverse movement. The 3D support structure was also designed to occupy ~25% of the total volume, such that ~75% of the ‘open’ space is available for the cell-laden hydrogel. A computational rendering of the 3D support structure is shown in Figure 2A. From this rendering, a series of 2D digital images were created and used to generate light projections for the SLA process using a commercially available Autodesk Ember Printer which prints a proprietary and stable photopolymerizable resin (Autodesk, PR-48) at a resolution reported to be 50 μm. Top view and side view images of the 3D printed structure are shown in Figure 2B, which confirm successful printing of the 3D design.

Due to the hydrophobicity of the commercial resin that formed the printed structure, oxygen plasma treatment was investigated. A bulk printed material was made from the same resin and exposed to oxygen plasma. Increasing the time of treatment led to a decrease in the

water contact angle and thus an increase in hydrophilicity (Figure 2C). By three minutes of treatment, the water droplet nearly wet the surface resulting in a contact angel of 10 degrees indicating increased hydrophilicity. This condition was used for all subsequent experiments.

The ability to infill the 3D printed support structure with a hydrogel was investigated (Figure 3). A precursor solution of 8-arm norbornene functionalized PEG monomer (10kDa), a PEG dithiol crosslinker (1kDa), and fluorescently labeled PEG monothiol (1kDa) in the presence of a maleimide-conjugated fluorophore was infilled into the 3D printed construct and photopolymerized. Successful infilling of the PEG hydrogel was demonstrated by confocal microscopy (Figure 3A). A top view of the 3D printed structure shows the infilled hydrogel surrounding the pillars of the support structure. To demonstrate distribution of the cells in the PEG hydrogel infill, fluorescently-labeled microspheres (10 μm diameter) of similar size to cells were suspended in the hydrogel precursor solution, injected into the support structure and then exposed to light (Figure 3B). Representative confocal microscopy images confirm a relatively uniform distribution of the microspheres within the void spaces of the support structure.

With the long-term goal being to use the hybrid scaffold to treat focal chondral defects, the hybrid scaffold was investigated for its ability to support chondrocytes and cartilage-specific ECM synthesis. Freshly isolated chondrocytes were suspended in a hydrogel precursor solution, injected into the support structure, exposed to light to entrap the cells within the hybrid scaffold and then cultured for two weeks (Figure 3C). In these studies, a degradable PEG hydrogel was used where the crosslinker was a matrix metalloproteinase 2 (MMP2) sensitive peptide crosslinker.[37] This particular crosslinker was chosen because chondrocytes have been shown to secrete MMP2 during cartilage development and remodeling.[38,39] Confocal microscopy images confirm that chondrocytes were entrapped in the hydrogel regions surrounding the support structure (Figure 3C). Chondrocyte phenotype and ECM synthesis was confirmed by staining for collagen type II, which is one of the main cartilage-specific ECM proteins found in cartilage (Figure 3C). These findings demonstrate the feasibility of delivering chondrocytes in a degradable hydrogel into a 3D printed support structure and their ability to produce cartilage-specific ECM.

The hybrid scaffold was tested in an *ex vivo* focal chondral defect to demonstrate the ability to fill the defect *in situ* and to investigate the surrounding cartilage once filled in a dynamic mechanical environment. A chondral defect was prepared in osteochondral plugs explanted from the trochlear groove of adult porcine knees (Figure 4). The 3D printed support structure was treated with oxygen plasma, physically placed into the focal chondral defect, infilled with a hydrogel precursor solution, and photopolymerized *in situ* (Figure 4A). To assess the ability of the *in situ* hybrid scaffold to protect the surrounding tissue from further damage, a stable version of the hydrogel was employed to minimize confounding factors that could arise due to changes in the scaffold properties. To emulate the *in vivo* environment, the osteochondral plugs (filled and empty) were subjected to physiologically relevant dynamic compressive strains for one hour per day for three weeks in custom built bioreactors (Figure 4A). The loading profile consisted of an 10% offset strain followed by a 2% peak to peak dynamic loading strain, which has been previously shown to maintain cartilage explants *ex vivo* (Figure 4B).[40] Photographs show an unfilled defect and a defect

filled with the hybrid scaffold immediately after filling (Figure 4C). The osteochondral plugs were cultured for four weeks under free swelling or dynamic loading conditions and then removed, visualized, and then processed for histology.

All hybrid scaffolds filling the defects visually remained in place in both loading and free swelling culture conditions after four weeks. The surrounding tissue was characterized by staining for sulfated glycosaminoglycans (sGAGs), which are the main GAGs found in aggrecan, the most abundant proteoglycan in cartilage, and have been shown to be the first ECM molecule that is lost during early stages of cartilage degeneration (Figure 4D).[41] Our results reveal that chondral defects left untreated displayed depletion of sGAGs in the regions adjacent to the defect (~140 μm from edge of defect), indicative of degeneration (Figure 4E). However, chondral defects that were treated with the hybrid scaffold showed significantly higher retention of sGAGs in the regions adjacent to the defect, regardless of the loading environment (Figure 4D and 4E). These results demonstrate that infilling of the defect with the hybrid scaffold prevents degeneration of cartilage adjacent to a defect regardless of the presence of loading. Although the exact mechanism is not known, the physical confinement that results from *in situ* polymerization of the infilled hydrogel may prevent tissue swelling along the defect boundary and protect the tissue.[42] Additional studies, however, are needed to elucidate the mechanisms involved.

Herein, we demonstrate the applicability of combining stereolithography with injectable hydrogels to create a new hybrid scaffold for treating focal defects in cartilage. 3D printing strategies have been investigated for cartilage tissue engineering with the most common method being extrusion-based printing.[43–45] Although promising, the resolution of the bioprinted material is restricted by nozzle size, polymer viscosity, and printing speed, limiting the choice of material and the resolution of the printed structure.[43,45–47] Stereolithography, on the other hand, achieves higher resolution and can be applied to essentially any photopolymerizable monomer solution,[33,43,46] thus, enabling structures to be printed at relevant lengthscales and properties that mimic native tissues (e.g., zonal regions within cartilage). A few studies have investigated stereolithography in cartilage tissue engineering to create 3D porous scaffolds, but have only investigated seeding chondrocytes directly onto the scaffold. [48,49] Also, little is known on the applicability of the 3D printed structures in chondral defects with physiologically relevant mechanical loading. In this work, we introduced a novel approach that leverages the advantages of stereolithography to create complex 3D architectures and simultaneously the advantages of injectable synthetic-based hydrogels for chondrocyte delivery and for ease of placement and *in situ* polymerization into chondral defects.

There are several limitations of this study. The resolution and mechanical properties of the 3D printed support structure were limited to the commercial resin, which is not designed to degrade, and the SLA 3D printing process. Moreover, under dynamic loading the *in situ* filled OC defect creates a complex mechanical environment due to several factors such as the confinement of the scaffold by the adjacent cartilage and the bond between the infilled hydrogel and the adjacent cartilage. To address these limitations, future work will use a custom-built SLA 3D printer,[50] which has a resolution of 4 μm and which can be used with a wide range of polymer formulations to tune the degradation (e.g., with enzymatically and/or

hydrolytically cleavable sites) and mechanical properties of the support structure. Other advanced 3D printing technologies have also been developed with enhanced resolution capabilities.[51] Future work will also implement computational methods[52] to characterize the complex mechanical properties of the hybrid scaffold within the defect. Another limitation of this study was the mechanical loading environment in the explant osteochondral model, which was limited to compressive strains. In the *in vivo* environment, understanding the effect of shear strains combined with compressive strains will be important.

3. Conclusions

In summary, treating focal defects in articular cartilage is a significant challenge clinically. Many current approaches still rely on a single scaffold, which limits the functions that the scaffold can perform *in vivo.*[53] Thus, there is a need in tissue engineering to develop more complex 3D scaffolds that have structural integrity and clinically relevant biological functions for supporting tissue regeneration and maintaining the tissue surrounding the implanted scaffold.[32] We present in this proof of concept study, a hybrid scaffold that combines *in situ* delivery of chondrocytes within a hydrogel, but which is supported through an embedded 3D printed structure. Our approach enables independent design of the support structure and the hydrogel such that in the future the hydrogel can be designed to degrade rapidly while the support structure can be designed to degrade slowly. Importantly, this study demonstrates that a hybrid scaffold maintains the health of the surrounding tissue. Long-term, this approach can be adapted using minimally invasive methods to repair focal chondral defects where imaging modalities, such as MRI, could be used to size the 3D printed support structure prior to surgery. Overall, this feasibility study presents a new hybrid scaffold approach as a potential therapy to treat focal defects and prevent cartilage degeneration long-term and warrants further research.

4. Experimental Section

4.1. Fabrication of the 3D support structure by SLA-based 3D printing

Solidworks® was used to generate a 3D model of the support structure made of an array of 250 μm diameter pillars evenly spaced to achieve a 25% volume fraction. A 250 μm thick lattice was then added at the top, middle and bottom to provide lateral support. The dimensions of the structure were 2.06 × 2.06 × 2.00 mm (L × W × H). Autodesk's Print Studio software was used to generate 10 μm thick 2D slices from the 3D model. The 2D digital image slices were uploaded to the Autodesk Ember projection SLA printer, which is optimized for printing 10 μm thick layers. In brief, the build head is lowered into a resin bath a distance of 10 μm from the printing window, whereby a 2D digital image is projected to polymerize the resin in regions exposed to light. The process is repeated layer-by-layer until the full 3D structure is complete. A separate single layer bulk material was printed following the same polymerization conditions and used for the contact angle experiments. The commercial resin for the Autodesk Ember projection SLA printer was used. The 3D printed support structure was removed, soaked in isopropanol for 15 min to remove monomer from the unexposed regions and then sterilized in 70% ethanol overnight followed by drying under sterile conditions.

4.2. Oxygen plasma treatment of the 3D printed support structures

Following aseptic protocols, the oxygen plasma chamber (Plasma Etch Inc., PE-25) was sterilized and stabilized by purging the chamber with oxygen plasma for 15 minutes. The sterile samples were transferred in sterile tissue culture plates, placed in the chamber, and then exposed to oxygen plasma for 1, 2 or 3 minutes. The treated materials (either the 3D printed support structure or the bulk printed material) were used immediately. The bulk printed materials were tested for hydrophilicity by photographing a water droplet on the surface.

4.3. Infilling of 3D printed support structures with a PEG hydrogel

A PEG hydrogel was formed from precursor solution of 10 (g/g)% 8-arm PEG (10kDa) norbornene, which was synthesized from 8-arm PEG (10kDa) amine following established protocols,[35] PEG (1kDa) dithiol at a 1:1 thiol:ene ratio, and 0.05 (g/g)% photoinitiator Igracure 2959 (I2959) (BASF) in phosphate buffered saline (PBS). The hydrogel precursor solution was injected into the 3D printed support structure under vacuum and polymerized with 352 nm light at 5 mW cm^{-2} for 10 minutes. The hybrid scaffold was swollen to equilibrium for 24 hours in PBS prior to characterization. To image the hydrogel in the hybrid scaffold, 0.1 (v/v)% Alexa-Fluor 546 maleimide (Thermo Fisher Scientific) was added to the precursor solution prior to polymerization. In a separate experiment, Alexa-Fluor 546 labeled microspheres (10μm) (FluoSpheres, Molecular Probes) at 1 million spheres per ml of precursor solution were infilled and photopolymerized. In both, the swollen hybrid scaffold was imaged by confocal microscopy (Zeiss LSM 5 Pascal). 3D printed constructs were sectioned using a razor blade to image infilling in the center of the 3D printed constructs.

4.4. Infilling a cell-laden hydrogel in 3D printed constructs

Bovine chondrocytes were isolated from the femoral-patellar groove of a skeletally immature (1–3 weeks old) calf (Arapahoe Meat Co., Lafayette, CO) following established protocols.[35] Bovine chondrocytes were suspended in the 0.22 μm sterile filtered hydrogel precursor solution at 50 million cells/ml in a 10 (g/g)% 8-arm PEG (20kDa) norbornene, with a matrix metalloproteinase (MMP2) degradable peptide crosslinker (GCVPLSLYSGCG) at a 1:1 thiol:ene ratio. This solution was injected into the 3D printed support structures under vacuum for 30 seconds, and photopolymerized for 8 minutes at 352nm at 5 mW cm^{-2}. The cell-laden hydrogels were cultured in chondrocyte medium (DMEM supplemented with 10% FBS, 0.2% Primocin, 10 mM HEPES, 0.1 M non-essential amino acids, 50 μg ml^{-1} L-ascorbic acid, 4mM l-glutamine, 0.4μM l-proline) for up to 14 days (n=3). Cell-laden hydrogels were fixed in 4% paraformaldehyde for 24 hours at 4°C and were processed for histology following standard protocols. Sections (40 μm) were pretreated with 200 U ml^{-1} hyaluronidase for 1 hour at 37°C, followed by permeabilization (0.25% Triton X, 1% BSA in PBS) and blocking (1% BSA), treatment with an anti-collagen II primary antibody (1:50) (abcam ab3092) overnight at 4°C, treatment with Alexa-Fluor 488 conjugated secondary antibodies, and treatment with DAPI. Images were taken using confocal microscopy (Ziess LSM 5 Pascal).

4.5. *Ex vivo* focal defect treatment of osteochondral plugs

Osteochondral plugs (8mm diameter, 10 mm deep) were explanted from the trochlear groove of porcine knees following aseptic protocols. Focal chondral defects (3mm diameter, ~2mm deep) were created in the center of the osteochondral plug. The inside of the chondral defect was dried using sterile filtered (0.2μm syringe filter) CO_2 for 1 minute. The 3D printed support structure was placed into the chondral defect site, and a 0.22 μm sterile filtered hydrogel precursor solution (10wt% 8-arm PEG norbornene (10kDa), PEG dithiol (1kDa) at 1:1 thiol:ene ratio, 0.05wt% I2959) was injected into the 3D printed support structure, subjected to vacuum for 2 minutes and polymerized (352 nm, 5mW cm^{-2} for 8 minutes). A separate set of osteochondral plugs were left empty. Filled and empty plugs were cultured in chondrocyte media under either a) free swelling for 4 weeks (filled n=4, empty n=4) or b) free swelling conditions for 1 week followed by 3 weeks of unconfined dynamic compression in a custom bioreactor (filled n=4, empty n=4).[54,55] In the latter, specimens were held at a constant strain of 2.5% throughout the culture, but for one hour per day were subjected to a 10% offset strain onto which a 2% peak to peak strain at 1Hz in a sinusoidal waveform was applied. Each plug was cultured individually in a 24-well plate with 2ml per well of chondrocyte media which was replaced every other day. After four weeks, the cartilage layer was removed from the bone layer, fixed in 10% formalin for 2 days at room temperature, transferred to 70% ethanol for storage and then were processed for histology following standard protocols. Sections (20μm) were stained for sGAGs by Safranin O and fast green and imaged by light microscopy. Semi-quantitative analysis of histological images was performed in which measurements of the width of degenerated tissue defined by a lack of red stain were taken (n=10 measurements per image, 5 images per sample, 4 samples per condition).

Acknowledgments

Research reported in this publication was supported by the National Institute of Arthritis and Musculoskeletal and Skin Diseases of the National Institutes of Health under Award Number 1R01AR069060. The content is solely the responsibility of the authors and does not necessarily represent the official views of the National Institutes of Health. The authors acknowledge the Department of Education's Graduate Assistantship in Areas of National Need to EAA. The authors acknowledge Karin Payne and Francisco Fontan for their assistance in creating the osteochondral plugs and Stanley Chu and Margaret Schneider for their assistance in isolating bovine chondrocytes.

References

1. Buckwalter JA, Brown TD. Clin Orthop. 2004; 423:7–16.
2. Buckwalter JA, Mankin HJ, Grodzinsky AJ. Instr Course Lect. 2005; 54:465–480. [PubMed: 15952258]
3. Fick JM, Thambyah A, Broom ND. Connect Tissue Res. 2010; 51(2):132–149. [PubMed: 20001847]
4. Mithoefer K, McAdams T, Williams RJ, Kreuz PC, Mandelbaum BR. Am J Sports Med. 2009; 37(10):2053–2063. [PubMed: 19251676]
5. Steadman JR, Rodkey WG, Rodrigo JJ. Clin Orthop. 2001; 391:S362–369.
6. Redman SN, Oldfield SF, Archer CW. Eur Cell Mater. 2005; 9:23–32. [PubMed: 15830323]
7. Gill TJ, Asnis PD, Berkson EM. J Orthop Sports Phys Ther. 2006; 36(10):728–738. [PubMed: 17063835]
8. Visna P, Pasa L, Cizmar I, Hart R, Hoch J. Acta Chir Belg. 2004:709–14. [PubMed: 15663280]

9. Knutsen G, Drogset JO, Engebretsen L, Grontvedt T, Isaksen V, Ludvigsen TC, Roberts S, Solheim T, Strand O, Johansen E. j Bone Joint Surge Am. 2007; 89(10):2105–12.
10. Gillogly SD, Myers TH. Orthop Clin North Am. 2005; 36(4):433–446. [PubMed: 16164949]
11. Bartlett W, Skinner JA, Gooding CR, Carrington RWJ, Flanagan AM, Briggs TWR, Bentley G. J Bone Joint Surg Br. 2005; 87(5):640–645. [PubMed: 15855365]
12. Kraeutler MJ, Belk JW, Purcell JM, McCarty EC. Am J Sports Med. 2017 363546517701912.
13. Gooing CR, Bartlett W, Bentley G, Skinner JA, Carrington R, Flanagan A. Knee. 2006; 13(3):203–10. [PubMed: 16644224]
14. Huey DJ, Hu JC, Athanasiou KA. Science. 2012; 338(6109):917–921. [PubMed: 23161992]
15. Temenoff AG, Mikos JS. Biomaterials. 2000; 21(5):431–440. [PubMed: 10674807]
16. Grande DA, Halberstadt C, Naughton G, Schwartz R, Manji R. J Biomed Mater Res. 1997; 34(2): 211–220. [PubMed: 9029301]
17. Chen FH, Rousche KT, Tuan RS. Nat Rev Rheumatol. 2006; 2(7):373–382.
18. Kuo CK, Li W-J, Mauck RL, Tuan RS. Curr Opin Rheumatol. 2006; 18(1):64–73. [PubMed: 16344621]
19. Drury JL, Mooney DJ. Biomaterials. 2003; 24(24):4337–4351. [PubMed: 12922147]
20. Nicodemus GD, Bryant SJ. Tissue Eng Part B Rev. 2008; 14(2):149–165. [PubMed: 18498217]
21. Elisseeff J, McIntosh W, Anseth K, Riley S, Ragan P, Langer R. J Biomed Mater Res. 2000; 51(2): 164–171. [PubMed: 10825215]
22. Bryant SJ, Anseth KS. Hydrogels J Biomed Mater Res. 2002; 59(1):63–72. [PubMed: 11745538]
23. Neumann AJ, Quinn T, Bryant SJ. Acta Biomater. 2016; 39:1–11. [PubMed: 27180026]
24. Burdick JA, Chung C, Jia XQ, Randolph MA, Langer R. Biomacromolecules. 2005; 6(1):386–391. [PubMed: 15638543]
25. Rice MA, Anseth KS. J Biomed Mater Res A. 2004; 70A(4):560–568.
26. Nicodemus GD, Skaalure SC, Bryant SJ. Acta Biomater. 2011; 7(2):492–504. [PubMed: 20804868]
27. Roberts JJ, Nicodemus GD, Greenwald EC, Bryant SJ. Clin Orthop. 2011; 469(10):2725–2734. [PubMed: 21347817]
28. Sridhar SL, Schneider MC, Chu S, de Roucy G, Bryant SJ, Vernerey FJ. Soft Matter. 2017; 13(28): 4841–4855. [PubMed: 28613313]
29. Zhang AP, Qu X, Soman P, Hribar KC, Lee JW, Chen S, He S. Adv Mater Deerfield Beach Fla. 2012; 24(31):4266–4270.
30. Tumbleston JR, Shirvanyants D, Ermoshkin N, Janusziewicz R, Johnson AR, Kelly D, Chen K, Pinschmidt R, Rolland JP, Ermoshkin A, Samulski ET, DeSimone JM. Science. 2015; 347(6228): 1349–1352. [PubMed: 25780246]
31. Zhu W, Ma X, Gou M, Mei D, Zhang K, Chen S. Curr Opin Biotechnol. 2016; 40:103–112. [PubMed: 27043763]
32. Kang H-W, Lee SJ, Ko IK, Kengla C, Yoo JJ, Atala AA. Nat Biotechnol. 2016; 34(3):312–319. [PubMed: 26878319]
33. Cooke MN, Fisher JP, Dean D, Rimnac C, Mikos AG. J Biomed Mater Res B Appl Biomater. 2003; 64B(2):65–69.
34. Fairbanks BD, Schwartz MP, Halevi AE, Nuttelman CR, Bowman CN, Anseth KS. Adv Mater Deerfield Beach Fla. 2009; 21(48):5005–5010.
35. Roberts JJ, Bryant SJ. Biomaterials. 2013; 34(38):9969–9979. [PubMed: 24060418]
36. Skaalure SC, Chu S, Bryant SJ. Adv Healthc Mater. 2015; 4(3):420–431. [PubMed: 25296398]
37. Amer LD, Holtzinger A, Keller G, Mahoney MJ, Bryant SJ. Acta Biomater. 2015; 22:103–110. [PubMed: 25913222]
38. Sternlicht MD, Werb Z. Annu Rev Cell Dev Biol. 2001; 17(1):463–516. [PubMed: 11687497]
39. Vu TH, Werb Z. Genes Dev. 2000; 14(17):2123–2133. [PubMed: 10970876]
40. Sah RL, Grodzinsky AJ. Biochem J. 1990; 267(3):803–808. [PubMed: 2339990]
41. Pritzker KPH, Gay S, Jimenez SA, Ostergaard K, Pelletier JP, Revell PA, Salter D, van den Berg WB. Osteoarthritis Cartilage. 2006; 14(1):13–29. [PubMed: 16242352]

42. Maldonando M, Nam J. Biomed Res Int. 2013:284873. [PubMed: 24069595]
43. Guo T, Lembong J, Zhang LG, Fisher JP. Tissue Eng Part B Rev. 2016
44. Cui X, Breitenkamp K, Finn MG, Lotz M, D'Lima DD. Tissue Eng Part A. 2012; 18(11–12):1304–1312. [PubMed: 22394017]
45. Klein TJ, Malda J, Sah RL, Hutmacher DW. Tissue Eng Part B Rev. 2009; 15(2):143–157. [PubMed: 19203206]
46. Schuurman W, Khristov V, Pot MW, van Weeren PR, Dhert WJA, Malda J. Biofabrication. 2011; 3(2):021001. [PubMed: 21597163]
47. Izadifar Z, Chen X, Kulyk W. J Funct Biomater. 2012; 3(4):799–838. [PubMed: 24955748]
48. Lee S-J, Kang H-W, Park JK, Rhie J-W, Hahn SK, Cho D-W. Biomed Microdevices. 2008; 10(2): 233–241. [PubMed: 17885804]
49. Schuller-Ravoo S, Teixeira SM, Feijen J, Grijpma DW, Poot AA. Macromol Biosci. 2013; 13(12): 1711–1719. [PubMed: 24214105]
50. Linnenberger A, Bodine MI, Fiedler C, Roberts JJ, Skaalure SC, Quinn JP, Bryant SJ, Cole M, McLeod RR. Opt Express. 2013; 21(8) 1-269-77.
51. Zhou F, Cao W, Dong B, Reissman T, Zhang W, Sun C. Advanced Optical Materials. 2016; 4:1034–104.
52. Kinneberg KRC, Nelson A, Stender ME, Aziz AH, Mozdzen LC, Harley BAC, Bryant SJ, Ferguson VL. Annals of Biomedical Engineering. 2015; 43(11):2618–29. [PubMed: 26001970]
53. Chang CC, Boland ED, Williams SK, Hoying JB. J Biomed Mater Res B Appl Biomater. 2011; 98(1):160–170. [PubMed: 21504055]
54. Nicodemus GD, Bryant SJ. J Biomech. 2008; 41(7):1528–1536. [PubMed: 18417139]
55. Villanueva I, Hauschulz DS, Mejic D, Bryant SJ. Osteoarthritis Cartilage. 2008; 16(8):909–918. [PubMed: 18203631]

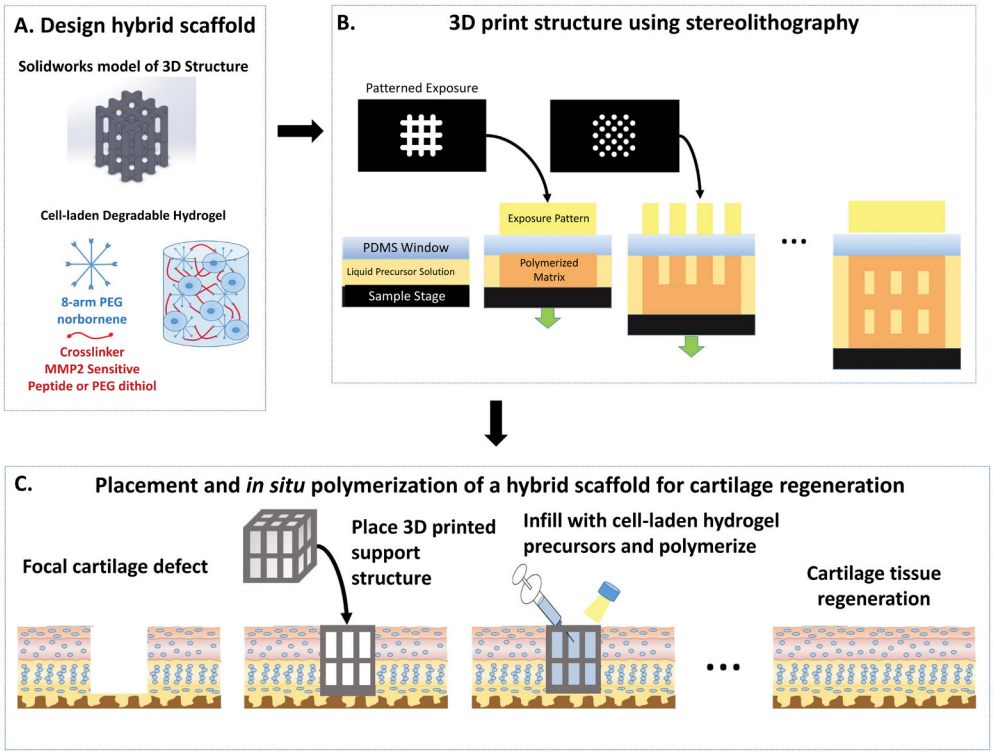

Figure 1.

A schematic of the design, development and application of a hybrid scaffold for the potential treatment of a focal defect in articular cartilage. The hybrid scaffold consists of a 3D printed support structure and a cell-laden hydrogel (A). The 3D structure is printed using stereolithography through layer-by-layer digital projection printing (B). The overall vision of our approach (C) is to treat a focal defect by placing the 3D structure into the defect, infilling with an aqueous solution of cells (e.g., cartilage cells) in a hydrogel precursor solution, followed by polymerization via light. Over time, the cell-laden hydrogel facilitates neotissue growth while the support structure maintains the mechanical integrity of the scaffold and ultimately both degrade leading to cartilage regeneration.

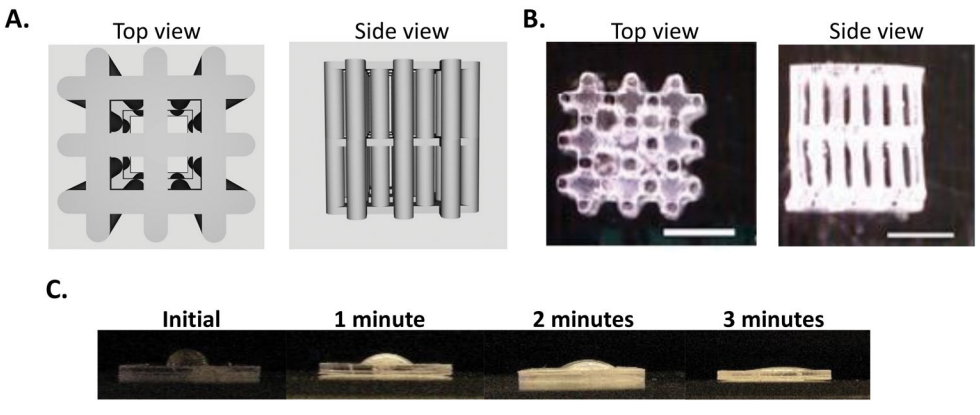

D.

Time of Treatment	Initial	1 minute	2 minutes	3 minutes
Contact Angle Measurements	78 (2)	43 (2)	31 (1)	10 (2)

Figure 2.

A. Solidworks® 3D drawings from the top and side of the 3D support structure with 250 μm diameter pillars and top, middle, and bottom lattice structures and occupying 25% volume fraction. B. Photographs of the SLA 3D printed structure from the top and side (scale bar is 1 mm). C. Photographs of water droplets on a bulk specimen made from the same material as the 3D support structure treated with oxygen plasma treatment for 0, 1, 2 and 3 minutes. A decrease in the water contact angle can be visualized with increasing oxygen plasma treatment. D. Contact angle measurements after oxygen plasma treatment. Data are represented as mean with standard deviation reported parenthetically for n=3.

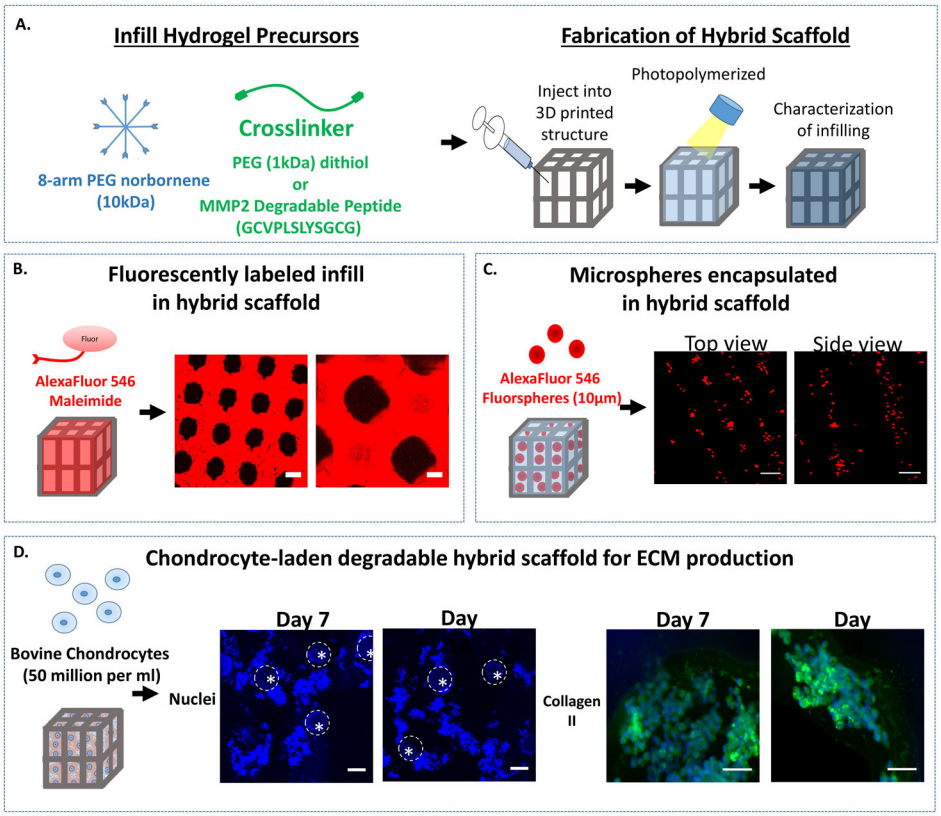

Figure 3.

A. A schematic of the photopolymerizable PEG precursor solutions for the infill and the fabrication of the hybrid scaffold by injecting the precursors and photopolymerizing. B. A schematic of the infilling of the hybrid scaffold with a fluorescently-labeled, PEG hydrogel. Representative confocal microscopy images shows successful infilling of the hydrogel (red) around the 3D printed support structure (black) (scale bar = 100 µm). C. A schematic of the infilling of the hybrid scaffold with fluorescently-labeled microspheres that are suspended in the infill solution and then subsequently photopolymerized to encapsulate them in the PEG hydrogel in the hybrid scaffold. Representative confocal microscopy images show the distribution of microspheres (red) through the top of the lattice (left) and a side view through the pillars (right) (scale bar= 100 µm). D. A schematic of the infilling of a chondrocyte-laden hybrid scaffold to which bovine chondrocytes were suspended in the infill solution and then subsequently photopolymerized to encapsulate them in the PEG hydrogel. Here a MMP2-sensitive PEG hydrogel was used. Cell nuclei (blue) shows chondrocytes are successfully infilled around the pillars (indicated by dotted line) of the hybrid scaffold at 7 and 14 days (scale bar = 100 µm). High magnification images of regions of high cell density where extracellular matrix neotissue is forming as shown by staining for collagen type II (green) and cell nuclei (blue) at 7 and 14 days (scale bar = 20 µm).

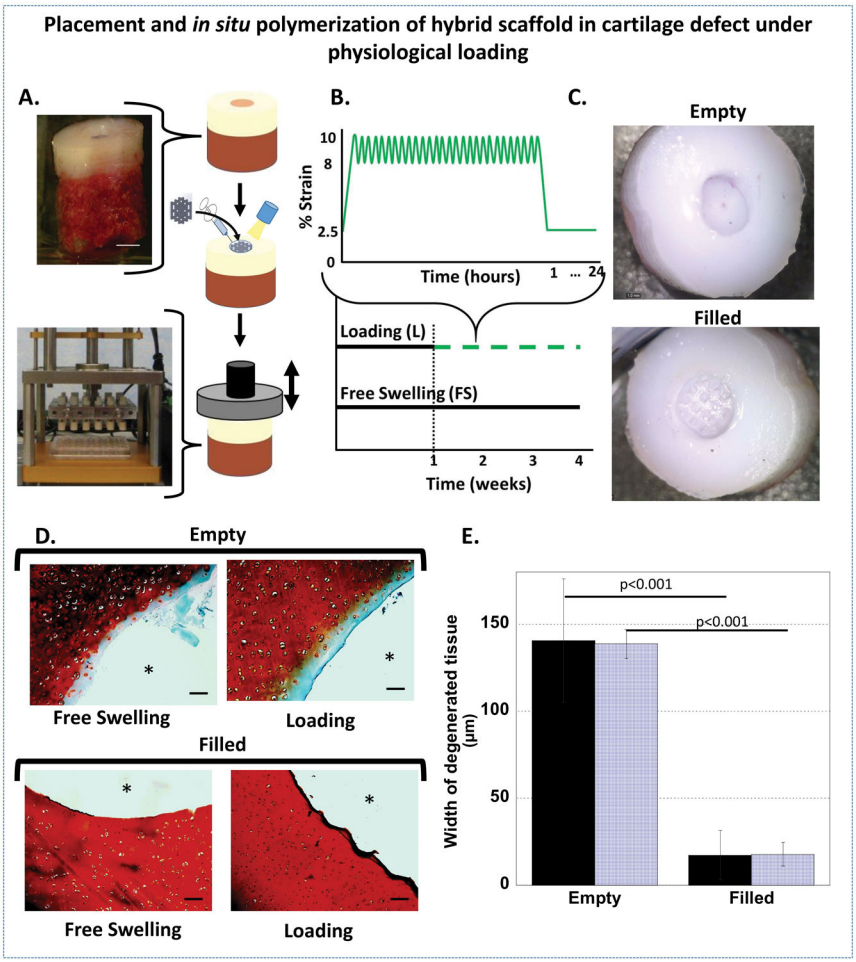

Figure 4.

A. A schematic showing the placement and infilling of the hybrid scaffold in a focal chondral defect of a porcine osteochondral plug (top) followed by intermittent, unconfined dynamic compression in custom bioreactors (bottom). B. A schematic of the intermittent dynamic loading profile (green, dashed) and free swelling (black, solid). Loading was applied by applying a slow ramp from the tare strain of 2.5% to 10% compressive strain followed by dynamic loading applied in a sinusoidal waveform at a frequency of 1 Hz between 8 and 10% compressive strain for one hour. A slow ramp was applied to remove the strain to 2.5% for 23 hours. C. Top view of osteochondral plugs with chondral defects that were left empty (top) and filled with the hybrid scaffold (bottom). Photographs were taken immediately after filling and prior to culture. D. Representative histological images of safranin O/fast green stained sections after 4 weeks show depletion of sGAGs (red) adjacent to the defect site in empty defects (* indicates empty defect site) and retention of sGAGs in the filled defects (* indicates hybrid scaffold) (scale bar = 100μm). E. The width of the degenerated tissue under free swelling (solid) and loading (striped) from semi-quantitative analysis of the sGAG histology (n=5, error bars = standard deviation).